Journal of Applied Electrochemistry (2006) 36:703–710
DOI 10.1007/s10800-006-9132-0

Influence of counter-ions on the permeability of polypyrrole films to hydrogen

P. HOLZHAUSER and K. BOUZEK*,†
*Department of Inorganic Technology, Institute of Chemical Technology, Technická 5, 166 28 Prague 6, Czech Republic (*author for correspondence E-mail: karel.bouzek@vscht.cz)*

Received 18 April 2005; accepted in revised form 27 January 2006

Key words: counter-ion, Nafion®, permeability, polypyrrole, proton exchange membrane fuel cell (PEM FC)

Abstract

The influence of the size and nature of counter-ions on the permeability of polypyrrole films to hydrogen was tested. The permeabilities were determined using the method of limiting currents on a Pt rotating disc electrode with subsequent Koutecky-Levich analysis. The work has focused mainly on the influence of the anion size, but the effect of polymeric anion hydrophilicity was also considered. Attention was especially paid to Nafion® as a counter-ion. It was found that Nafion® markedly increases polypyrrole permeability. The film growth was followed by means of EQCN, which allowed determination of the polypyrrole film densities.

List of symbols

b	Tafel slope (V decade^{-1})
c	molar concentration (mol cm^{-3})
C_{film}	solubility of H_2 (mol cm^{-3})
D	diffusion coefficient (cm^2 s^{-1})
f	frequency (kHz)
F	Faraday constant (C mol^{-1})
j	current density (mA cm^{-2})
k	permeability (mol cm^{-1} s^{-1})
K	constant Eq. (i) (cm^3 C^{-1})
K'	constant Eq. (xii) (g C^{-1})
m	weight (μg)
n	number of electrons exchanged
S	geometric surface area (cm^2)
Q	electric charge for film synthesis (C)
x_{EQCN}	calibration constant of crystal (μg kHz^{-1})

Greek symbols

δ	thickness (cm)
η	overvoltage (V)
P	degree of coverage
ρ	density (g cm^{-3})
υ	kinematic viscosity (cm^2 s^{-1})
ω	angular rotation rate (rad s^{-1})

Indices

ads	adsorption
dif	diffusional
ext	extrapolated
film	polymer film
kin	reaction kinetics

1. Introduction

Polypyrrole (PPy) is one of the most commonly studied conducting polymers (CPs) because of its relatively high chemical and electrochemical stability and its simple, reproducible preparation from aqueous solution. One such application is its use in specially designed electrodes for fuel cells (FCs).

One of the most important problems with low temperature FCs is catalyst utilization. The most effective electrocatalysts are based on Pt, Ru or other precious metals [1]. To lower the cost of the FC either a catalyst has to be found that is not based on precious metal or the total catalyst load has to be reduced. The first option does not seem to be realistic at the moment. This is mainly due to the highly corrosive environment of the FC. The second option seems to be more promising. Nowadays binary and more recently ternary alloys are studied in order to minimise catalyst poisoning by CO and thus reduce its load. Yet another option is to change the catalyst support in order to achieve a similar effect. The use of CPs [2] for this purpose has two advantages. The first is based on the unique physical properties of CPs. These materials exhibit the mechanical properties of polymers and at the same time the electronic conductivity typical of metals. For a catalyst in a hydrogen-oxygen FC to function effectively it is necessary to secure its contact with (i) the current collector, (ii) the proton conductor and (iii) the fuel. Since a CP in the oxidized state has both electronic and ionic conductivity [3, 4] and

†ISE member

a porous structure [5], it represents an ideal FC catalyst support. The second advantage is enhanced resistivity to CO poisoning [6] for a Pt catalyst in a CP matrix compared to a carbon support.

The idea is to prepare a 3D-structured electrode in which nanosized catalyst particles are distributed in the matrix of a CP composite. The electrode reaction occurs on the surface of the catalyst particles and in this way protons and electrons are produced. This means that a catalyst-modified PPy film would have good efficiency as an electrode only if it were permeable to molecular hydrogen and conductive to protons [2]. So far, however, the application of CPs as a catalyst support has mainly been tested using a model system. This consists of a CP film deposited on a rotating disk electrode (RDE) made of electrocatalytically inactive glassy carbon (GC) [7–10]. Pt is subsequently deposited cathodically. In the literature generally the porous structure of this composite is considered. For this reason, it is assumed that it acts as a 3D electrode [6, 11–13]. According to our previous results [9], only the surface of the composite is active. This concept of a CP-supported catalyst has already been tested for FC electrode reactions such as the reduction of oxygen [7, 8, 14] and oxidation of hydrogen [9, 15] or methanol [6, 10, 16]. The first studies on the application of CPs in the construction of a membrane-electrode assembly have only recently been published [17, 18].

In order to achieve a high degree of catalyst utilization, CP film has to be sufficiently permeable for the fuel and at the same time a good proton conductor. The nature and size of the counter-ion incorporated into the film during its synthesis has an important impact on both the electrochemical and mechanical, as well as on the ion exchange properties [3–5]. The ion exchange properties are directly connected to the proton conductivity of the film. The influence of counter-ions on PPy properties has been the subject of many studies [19]. Nevertheless, a general study of the impact of the type of counter-ion on the electrochemical properties of PPy with respect to its hydrogen permeability has not yet been published. The aim of this paper is to fill this gap. This information allows optimization of the synthesis of PPy as a catalyst support for a proton exchange membrane FC (PEM FC) and a more realistic assessment of the feasibility of this approach.

The following counter-ions were selected for PPy preparation:

(i) chloride and sulphate anions, representing small monovalent and divalent anions (in the following these samples are denoted as PPy/Cl^- and PPy/ SO_4^{2-}),
(ii) 4-tolylsulfonate (Tos), representing large, but not polymeric anions (denoted as PPy/Tos),
(iii) poly(4-styrenesulfonate) (PSS), representing a large polymeric anion (denoted as PPy/PSS),
(iv) Nafion®, representing a large polymeric anion with a hydrophobic polymer backbone and hydrophilic ion exchange groups (denoted as PPy/Naf). A composite of PPy and Nafion® is of particular interest for use in FC electrodes since the Nafion® membrane is commonly used as a solid electrolyte in PEM-type FC.

The electrochemical quartz crystal nanobalance (EQCN) method was used to follow the influence of the nature of the counter-ion on the density of the PPy film studied.

2. Data analysis

2.1. *Film thickness*

PPy film thickness is directly proportional to the charge Q consumed during electropolymerization. The real film thickness δ_{film} was taken from scanning electron microscopy (SEM) pictures and plotted against the charge consumed during synthesis. The linear regression provides the value of constant K in the following equation:

$$\delta_{film} = K\frac{Q}{S}, \tag{1}$$

where S is the film geometric area. Eq. (1) was used to evaluate the PPy film thickness.

2.2. *PPy permeability*

Well-established methods exist for the determination of permeability based on the diffusion of hydrogen through the membrane separating two gaseous or liquid phases [20]. These methods, however, are not the most appropriate for determining the permeability of the PPy film to be used as an electrode material for the FC. This is because hydrogen permeating through the PPy layer is oxidized on the catalyst surface to protons. Low permeability of the electrode material to protons results in their accumulation at the interface. This can result in an anodic shift in the equilibrium potential of the $2H^+/H_2$ and consequently to deterioration of the FC voltage efficiency. Such local increase of pH would probably result in a PPy degradation. The classical diffusion method does not account for this fact.

For this particular application the RDE method developed by Lamy et al. [15] is more suitable. This method gives the PPy film permeability to hydrogen and also indicates the effect of low proton-conductivity. Permeability to hydrogen can be evaluated on the basis of limiting current density values. This method permits testing of the PPy film under conditions closer to the situation in the FC than an investigation of freestanding films.

To analyse the potentiostatic polarization curves, we have to distinguish between all the consecutive steps influencing the kinetics of the overall process of hydrogen oxidation on the PPy-modified Pt RDE. These steps are as follows: (i) diffusion of hydrogen from the bulk solution to the surface of the PPy film, (ii) diffusion of hydrogen through the PPy film, (iii) adsorption of hydrogen molecules on the Pt electrode surface and

finally (iv) oxidation of hydrogen on the Pt surface to protons. Thus, the current density flowing through the working electrode can be described as follows:

$$\frac{1}{j} = \frac{1}{j_{\text{dif}}} + \frac{1}{j_{\text{film}}} + \frac{1}{j_{\text{ads}}} + \frac{1}{j_{\text{kin}}}, \tag{2}$$

where the individual terms on the right-hand side are related to the above points (i) to (iv), respectively.

The mechanism of hydrogen oxidation with adsorption and oxidation steps is considered here because the reaction is carried out in a strongly acidic environment.

Adsorption and oxidation of hydrogen:

$$H_2^{(\text{film})} \rightarrow 2H^{(\text{ads})}, \quad \text{current density } j_{\text{ads}} \tag{3}$$

$$H^{(\text{ads})} \rightarrow H^{+(\text{film})} + e^-, \quad \text{current density } j_{\text{kin}}. \tag{4}$$

For hydrogen oxidation, the kinetic contribution can be described as follows [15]:

$$\frac{1}{j_{\text{kin}}} = \frac{1}{j_0} \cdot \frac{1}{\theta e^{\frac{\eta}{b}}}, \tag{5}$$

where j_0 is exchange current density for reaction (4), η the overvoltage, θ the degree of coverage of the Pt surface by molecular hydrogen (Eq. (3)) and b the Tafel slope. At overvoltages greater than 100 mV the term $1/j_{\text{kin}}$ becomes negligible [15].

In Eq. (2) only the j_{dif} term is dependent on the electrode rotation rate and can be described by the Levich equation (6):

$$j_{\text{dif}} = 0.62nFD^{\frac{2}{3}}\omega^{\frac{1}{2}}\upsilon^{-\frac{1}{6}}c_0, \tag{6}$$

where n, F and D have their usual electrochemical meaning, ω is the angular rotation rate, υ the kinematic viscosity of the solution and c_0 the bulk concentration of hydrogen. From Eq. (6) it is evident that j_{dif} is a linear function of $\omega^{\frac{1}{2}}$. Using the Koutecky-Levich plot (j^{-1} vs. $\omega^{-\frac{1}{2}}$) the influence of the mass transport through the Nernst diffusion layer can be eliminated by extrapolating $\omega^{-\frac{1}{2}} \rightarrow 0$ *i.e.* $1/j_{\text{dif}}$ to zero.

This extrapolated value can be written as:

$$\lim_{\omega \rightarrow \infty} \frac{1}{j} = \frac{1}{j_{\text{ext}}} \tag{7}$$

The diffusional (j_{film}) and adsorptive (j_{ads}) contributions in Eq. (2) must be distinguished. The diffusion of hydrogen through the PPy film can be described by the modified Fick law as follows:

$$j_{\text{film}} = -nFD_{\text{film}}\frac{C_{\text{film}}}{\delta_{\text{film}}}, \tag{8}$$

where C_{film} is the solubility of hydrogen in the PPy film and δ_{film} is the film thickness. Then the permeability k is defined by:

$$k = D_{\text{film}}\, C_{\text{film}} \tag{9}$$

Now

$$\frac{1}{j_{\text{ext}}} = \frac{\delta_{\text{film}}}{nFk} + \frac{1}{j_{\text{ads}}} \tag{10}$$

One way to determine the $1/j_{\text{ads}}$ term consists in taking measurements at the pure Pt electrode without PPy film. In such a case $1/j_{\text{film}} = 0$ and j_{ads} is then equal to j_{ext}. Since the value of j_{ads} is very sensitive to the conditioning of the Pt surface it is not stable in the long term. Moreover, the question of the influence of the PPy deposited on the Pt surface on j_{ads} value remains open.

If the data for different PPy film thickness δ_{film} are available a more precise and accurate means of j_{ads} evaluation is possible. By plotting the values $1/j_{\text{ext}}$ obtained by Koutecky-Levich analysis against thickness δ_{film} a linear dependence which intercepts the abscissa at $1/j_{\text{ads}}$ is obtained. The slope of the regression line permits the determination of permeability k, see Eq. (10). The latter method was used in this work.

2.3. *EQCN density determination*

The EQCN is a sensitive instrument for observing both the electrochemical and mass response of the system studied. The change in shear mode resonant frequency of a quartz crystal is directly proportional to its surface mass change. This is described by the Sauerbrey equation [21], often simplified for routine work to Eq. (11).

$$\Delta m = -x_{\text{EQCN}}\Delta f \tag{11}$$

The value of constant x_{EQCN} has to be determined experimentally.

The simple plot of surface mass change connected with PPy film formation vs. consumed electrical charge can be constructed. From the slope K' the film density can be determined using Eq. (12):

$$\rho = \frac{\Delta m}{S\delta_{\text{film}}} = \frac{K'}{K} \tag{12}$$

3. Experimental

The electrochemical measurements for permeability determination were performed using a three-electrode configuration in a gas-tight thermostated Simax glass cell. A HEKA potentiostat-galvanostat PG310 was used. All potentials refer to SCE if not otherwise indicated. A smooth Pt foil was used as a counter-electrode.

All the chemicals were of analytical purity grade and were used as received except for pyrrole (Py), which was freshly redistilled. The commercially available 5 wt. % solution of Nafion® from Aldrich was used. All solutions were prepared from demineralized water with conductivity of 0.5 μS cm^{-1} or lower.

A Pt RDE with a geometric area of 0.196 cm^2 was applied as a substrate for the PPy film synthesis. Prior to

the experiment it was polished with P4000 grinding paper to mirror finish and was washed with demineralized water. Subsequently the electrode was potentiodynamically cycled in 0.5 M H_2SO_4 until a reproducible curve of Pt in acidic environment was obtained.

In all cases the PPy films were prepared potentiostatically at 0.75 V from 0.1 M aqueous solution of Py with different supporting electrolytes: 0.1 M NaCl, 0.1 M Na_2SO_4, 0.1 M NaTos, 0.1 M NaPSS (related to the monomer unit). In the case of Nafion® the solutions for synthesis were prepared by mixing a given volume of commercial 5 wt. % solution of Nafion® in isopropyl alcohol with an aqueous solution of Py; the final volume was 5 ml and total Py concentration 0.1 M. The content of the Nafion® solution was varied from 10 to 70 vol. %. The temperature was kept constant at 20 °C; the thickness of the film was controlled by the charge passed during electropolymerization and subsequently determined from the SEM data. The thickness of the film ranged from 0.1 to 3.1 μm.

After film synthesis the modified electrode was washed with water, immersed in deaerated 0.5 M H_2SO_4 (or 1 M HCl) and purged for 20 min with nitrogen. The film was subsequently cycled 20 times between −0.2 and 0.5 V at a sweep rate of 50 mV s^{-1}. The electrolyte was then saturated with hydrogen and the same polarization regime was applied to obtain a film with stable composition. The limiting currents were determined from potentiostatic polarization curves measured in the potential range −0.2 to 0.5 V with 0.1 V step at a rotation rate of 50–3000 rpm in hydrogen saturated solution at 20 °C.

After the voltammetric experiments, the PPy film was detached from the Pt substrate and a sample was prepared for SEM. A Hitachi S4700 field emission electron microscope was used to determine the thickness of the films.

Microgravimetry experiments were performed using an Elchema EQCN-700 nanobalance connected to a PS-205B potentiostat. The electrochemical cell used was made of Simax glass and equipped with a 10 MHz quartz crystal with a gold working electrode of 0.196 cm^2 glued in place by a silicon sealant. Gold was chosen in order to minimise the effect of surface oxide layer formation. The instrument was calibrated by electrodeposition of copper from a deaerated 5 mM solution of $CuSO_4$ in 0.5 M H_2SO_4 [22] at a constant current of 120 μA. The PPy films were synthesized galvanostatically from the above-mentioned solutions at a current of 500 μA for 40 s.

4. Results

4.1. *SEM experiments*

For the majority of counter ions their influence on the PPy film morphology is well known [23]. In the case of Nafion® as a counter-ion, however, we faced problems with the formation of inhomogeneous leaky film [9]. Therefore, the impact of Nafion® content in the synthesis solution on sample morphology was studied. It was found that in the case of 10 vol. % content of Nafion® solution in the total volume of the synthesis solution the film produced is disrupted by holes visible to the eye as tiny dots on the film surface. A typical view of these defects is given in Figure 1. The films synthesized from more concentrated Nafion® solutions are compact and smooth, as expected for a polymeric counter-ion (see Figure 2).

The real thickness of films was evaluated from SEM images. Figure 3 shows linear plots of the dependence of film thickness on charge. The resulting values of K for Eq. (1) are summarized in Table 1.

4.2. *Film permeability*

Firstly, it was necessary to determine the optimal electrode potential for permeability measurement. The polarization curves for each type of film were measured with a potential step of 0.1 V in the range −0.2 to 0.5 V. Figure 4 shows typical polarization curves obtained. The low hydrogen oxidation current density observed at lower potentials is connected with the reduced PPy film. In the reduced state PPy film is shrunken and its hydrogen permeability deteriorates. An increase in the current density corresponds to the transition of PPy from the reduced to the oxidized state, which takes place in the potential range −0.1 to 0.1 V.

An alternative explanation is that PPy offers low permeability to protons formed at the Pt substrate. This, however, does not correspond to the fact that, in a reduced state, PPy film modified by polyanions (PSS and Nafion®) possesses cation selective properties [4]. Therefore these films should be more permeable to protons in the reduced than in the oxidized state. However, they exhibit hydrogen oxidation current

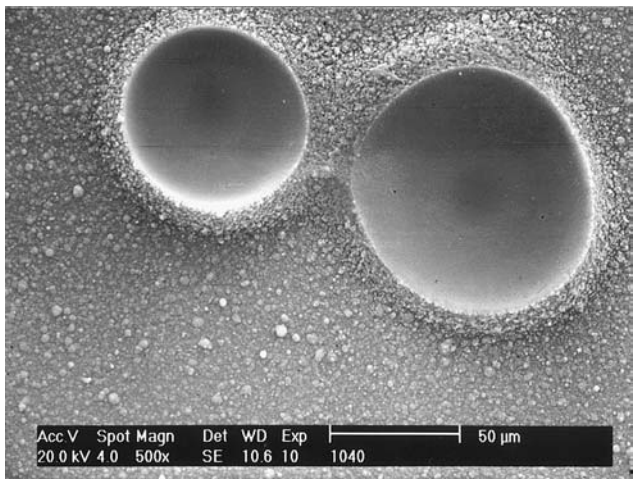

Fig. 1. SEM image of the holes in PPy/Naf film synthesised from a solution containing 10% of Nafion® solution, charge used for the film synthesis 1125 mC cm^{-2}.

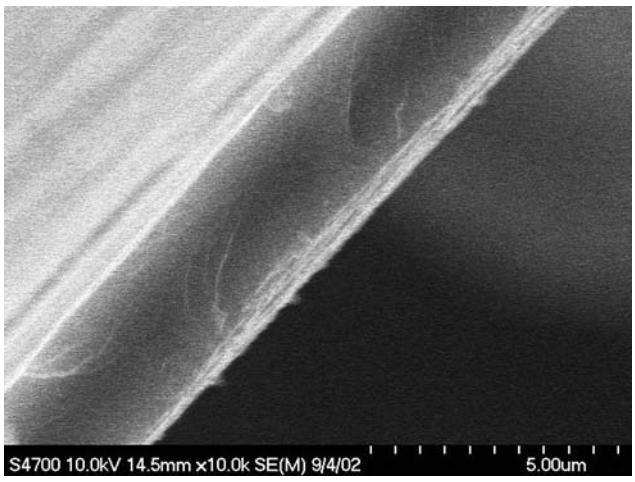

Fig. 2. SEM cross-section of PPy/Naf, 50%, charge used for the film synthesis 1125 mC cm^{-2}.

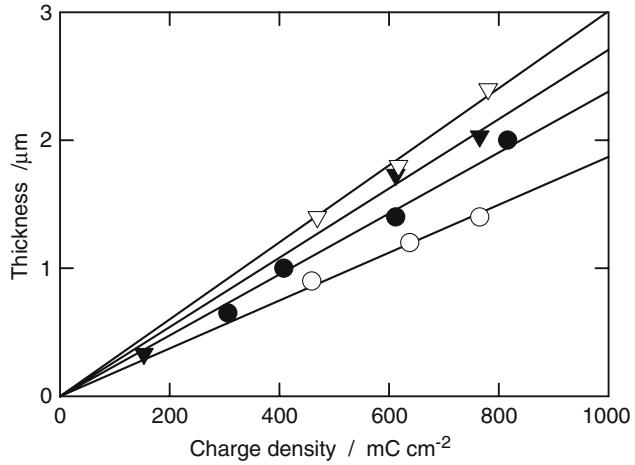

Fig. 3. Dependence of thickness of PPy film on charge density consumed during synthesis on GC electrode, ● PPy/Cl^-, ○ PPy/ SO_4^{2-}, ▼ PPy/Tos, ▽ PPy/PSS.

Table 1. Values of constants *K*, Eq. (1)

Counter-ion type	$10^4 \times K$ [cm^3 C^{-1}]
Chloride	2.37
Sulphate	1.86
Tosylate	2.70
Poly(styrenesulfonate)	3.00

density at low potentials comparable to the films with small counter-ions.

At higher potentials the surface of the electrode is modified by consecutive formation of Pt oxides. This influences the hydrogen adsorption process, thus modifying the catalytic properties of the Pt surface and lowering the current densities. In the majority of cases the maximum current density was observed at or close to a potential of 0.0 V. Therefore this potential was chosen for reading the current density values. The values of limiting current density were used to construct

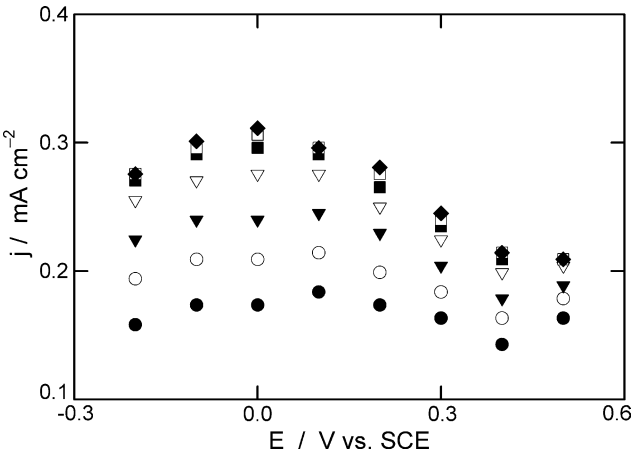

Fig. 4. Polarization curves of PPy/Naf (50%) modified Pt RDE in 0.5 M H_2SO_4 saturated with H_2 at 20 °C, film thickness $\delta_{film} = 3.1\ \mu m$, electrode rotation rate: ● 50 rpm, ○ 100 rpm, ▼ 200 rpm, ▽ 500 rpm, ■ 1000 rpm, □ 2000 rpm, ◆ 3000 rpm.

Koutecky-Levich plots (Figure 5). No change in the potential of hydrogen oxidation commencement was identified within the 100 mV step used to determine the potentiostatic polarisation curve. This indicates that no significant limitation by the PPy film permeability to protons occurred.

The first set of films was prepared with a chloride counter-ion. The results of the data evaluation differed from our theoretically based expectations. Figure 6 presents the dependence of extrapolated values of $1/j_{ext}$, taken from Koutecky-Levich plots (without correction for the adsorption step), on film thickness. According to Eq. (10) this value should ascend monotonically, but for films thicker than approximately 1 μm $1/j_{ext}$ decreases. This behaviour cannot be caused by a step in the hydrogen oxidation mechanism, because the rate-determining process can only change the value of the slope of the j_{lim} vs. *d* curve, but not its direction. The only explanation for the existence of an "inversion region"

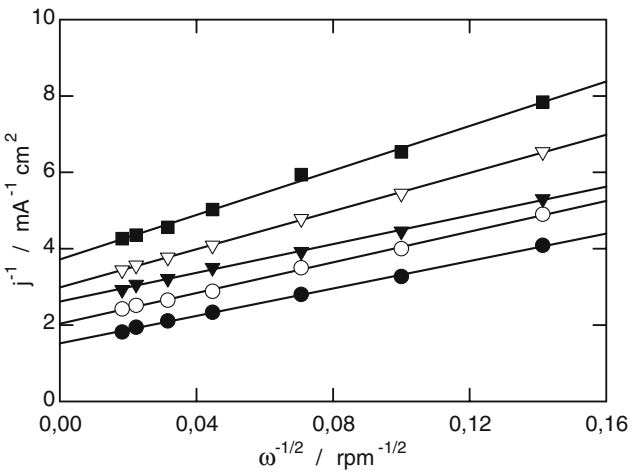

Fig. 5. Koutecky-Levich plots for PPy/PSS modified Pt RDE in 0.5 M H_2SO_4 saturated with H_2 at 20 °C, δ_{film}: ● 0.82 μm, ○ 1.17 μm, ▼ 1.41 μm, ▽ 1.85 μm, ■ 2.34 μm.

(where thicker films have higher permeability than thinner ones) is mechanical failure of the film. The explanation for this phenomenon is based on the assumption that chloride ions previously present in the PPy film are replaced by larger sulphate ions during potential cycling. This theory was proved by independent EQCN measurements. Here we observed a jump increase in PPy/Cl^- film mass within the first two potential cycles in sulphuric acid solution. This was caused by the exchange of lighter chloride for heavier sulphate ions. This is also in agreement with the observation of Michalska et al. [24] that the interaction of PPy/Cl^- film with sulphate ions leads to an accumulation of the latter in the film interior.

As the larger sulphate ions penetrate into the film interior the film is mechanically stressed and this results in the breakage and apparently higher permeability of thicker films.

Additional experiments were carried out to confirm this explanation. The effect of the exchange of different ions was excluded by using hydrochloric acid as an acidic medium for PPy/Cl^- permeability measurements. To obtain an identical concentration of protons a solution with a concentration of 1 M was used. Again the results are presented in Figure 6. No "inversion region" appears and the data can be evaluated according to the above-mentioned theory. The dependence of $1/j_{ext}$ on film thickness makes it possible to determine the $1/j_{ads}$ value and to calculate the permeability of the film.

Polarization curves of PPy films with the remaining counter-ions were measured in sulphuric acid solution. In this series of experiments, the effects of the exchange of different ions can be excluded. In the case of sulphate ion the anions present in the film and in the solution are identical. The remaining counter-ions (Tos, PSS and Nafion®) are fixed in the PPy film mechanically due to their size. No extraordinary behaviour was observed for any of these counter-ions. Data evaluation was identical to that of the PPy/Cl^- film.

Nafion® is of special interest as a counter-ion. For the construction of FCs with electrodes based on PPy, both the mechanical and the electrochemical compatibility of PPy film with a Nafion® membrane constitute an important factor. For this reason, the influence of the Nafion® content in a solution used for synthesis on PPy film permeability was studied. Figure 7 shows the dependence of film permeability on the composition of the synthesis solution. The permeability to 10 vol. % content is relatively high and is exceptional with respect to other experimental points. This is in good agreement with the SEM picture in Figure 1. The holes formed under these conditions cause hydrogen penetration to the Pt electrode surface, resulting in high hydrogen oxidation current densities, which lead to an unrealistically high apparent permeability value. From the course of the graph, it is possible to conclude that the permeability of PPy/Naf film increases with Nafion® content.

The contributions $1/j_{ads}$ determined and the permeability values obtained are summarized in Table 2.

4.3. *EQCN density determination*

Films were prepared galvanostatically and a total charge of 100 mC cm^{-2} was used in order to prepare PPy films of a defined constant thickness. The current density $j = 2.5$ mA cm^{-2} was set to ensure synthesis conditions close to the case of synthesis for RDE measurements. Figure 8 shows the dependence of mass change on the charge consumed during film growth. The linear dependence indicates homogeneous film growth and linearity of the EQCN crystal response. This fact indicates that the influence of the viscoelastic effect did not reach a significant level. Films of similar thickness and properties were obtained. Therefore any possible minor error introduced by the viscoelastic effect was similar for all samples studied and thus it had no influence on the

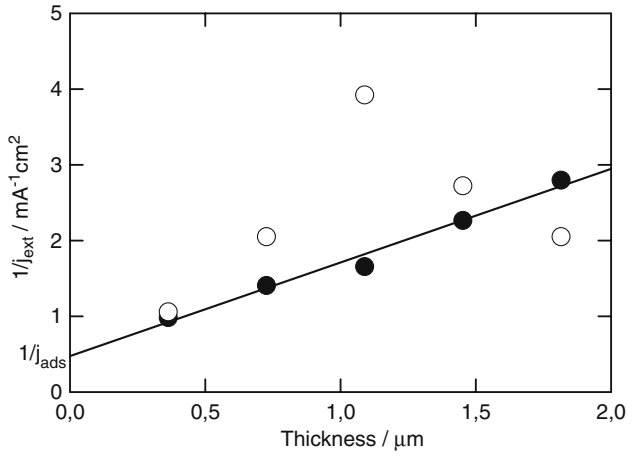

Fig. 6. Dependence of $1/j_{ext}$ values extrapolated from Koutecky-Levich plots on thickness of PPy/Cl^- film measured: ○ – in 0.5 M H_2SO_4 sat. with H_2 at 20 °C, ● – in 1 M HCl sat. with H_2 at 20 °C, used for determination of adsorptive term j_{ads}.

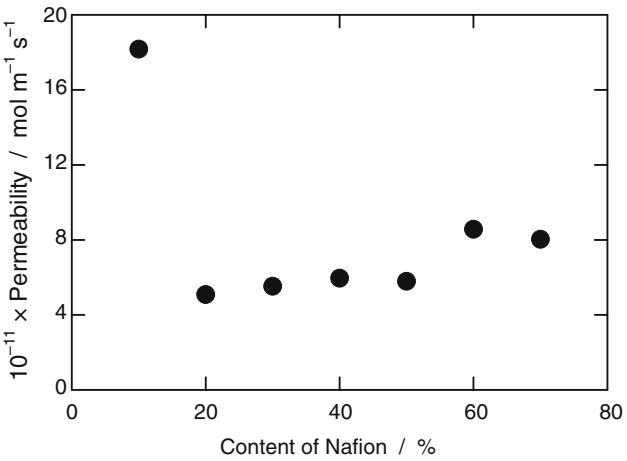

Fig. 7. Dependence of permeability of PPy/Naf film for H_2 on the content of Nafion® solution in the synthesis solution.

Table 2. Values of adsorptive contributions and permeabilities of PPy films

Counter-ion type	$1/j_{ads}$ [mA^{-1} cm^2]	$10^{13}\times k$ [mol cm^{-1} s^{-1}]
Chloride	0.473	4.16
Sulphate	~0	1.73
Tosylate	0.306	5.61
Poly(styrenesulfonate)	0.425	3.68
Nafion®, 70%	–	8.56

Table 3. Values of the slopes of curves from Fig. 8 and PPy film densities evaluated

Counter-ion type	$10^3\times K'$ [g C^{-1}]	ρ [g cm^{-3}]
Chloride	0.365	1.54
Sulphate	0.317	1.70
Tosylate	0.566	2.10
Poly(styrenesulfonate)	0.549	1.83

comparison of the densities of the PPy films. The correctness of the data is further proven by the quantitative agreement with literature data obtained, e.g. for PPy/Cl^- film [25]. The density of the film was calculated from the slopes K', see Figure 8, using Eq. (12); the results are summarized in Table 3. It is important to note that these data are related to a fully doped polymer with an oxidized backbone corresponding to a potential of ~0.75 V and a specific counter-ion.

5. Discussion

The PPy films prepared in the presence of large or even polymeric counter-ions were smooth, which is in agreement with the literature [23]. Polymeric Nafion® as a counter-ion also led to a compact film structure except for the 10 vol. % content in the synthesis solution. The smoother and more homogeneous films also have more mechanical resilience, which is important with respect to their use in FC.

Tables 2 and 3 contain the permeability and density values obtained. The densities of PPy film with different counter-ions (determined by the flotation method) are usually close to 1.5 g cm^{-3} [25]. The values determined in this work are slightly higher. The reason is that the thickness determined in the dry state differs slightly from the "wet" thickness of PPy in contact with the electrolyte. This is because, on drying, the PPy shrinks slightly. This leads to higher values of density. Nevertheless, this approach is often chosen [26]. A possible small systematic error does not influence the comparison of individual samples studied under identical conditions, which is the aim of this study.

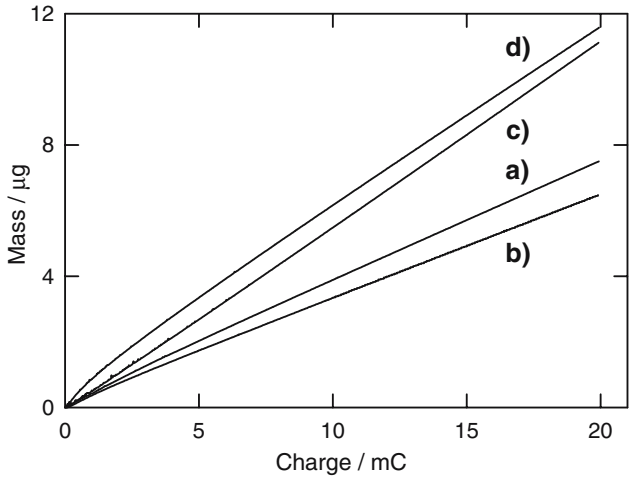

Fig. 8. Increase in mass of growing PPy films in dependence on the consumed charge, a) PPy/Cl^-, b) PPy/ SO_4^{2-}, c) PPy/Tos, d) PPy/PSS.

PPy/ SO_4^{2-} film exhibits a higher density of 1.70 g cm^{-3} and lower permeability as compared to PPy/Cl^-. Both these findings can be explained by the fact that a sulphate anion is a relatively small, divalent ion. It is believed that, in the oxidized state, the film shrinks in the presence of sulphate ions due to electrostatic interactions. This leads to a more compact structure, higher density and lower permeability. PPy/Tos and PPy/PSS films also have quite high densities (2.10 and 1.83 g cm^{-3}). The probable explanation is the similar nature of the Py units of the polymer and benzene rings of the counter-ions. The compatibility of molecules can produce favorable interactions and a denser steric arrangement. However, on the other hand the permeability values are closer to those of PPy/Cl^- than of PPy/ SO_4^{2-}.

The permeability of PPy film prepared from a solution with 70 vol. % of Nafion® solution is about twice that of PPy/Cl^-. The reason is not the polymeric character of the Nafion® anion, as experiments with PSS confirm. This increase can be explained by the characteristic structure of Nafion®. A pure Nafion® polymer exhibits permeability of 1.22×10^{-11} mol cm^{-1} s^{-1} [27]. This polymer consists of two different domains – hydrophilic and hydrophobic. The hydrophilic domain is formed by highly polar and hydrated sulphonic moieties, the hydrophobic domains are spread along the perfluorinated chains of the polymer backbone. The incorporation of hydrophobic chains thus improves the permeation of molecular hydrogen and the presence of hydrophilic areas facilitates the conduction of protons. These effects lead to increased permeability of the PPy/Naf composite. Nevertheless, it still remains one order of magnitude lower than for pure Nafion®, which in FC technology is considered to be practically impermeable to hydrogen. This finding supports our previous results [28] that the CP composites with cathodically deposited Pt behave as 2D-electrodes. This is caused by the low permeability of PPy to fuel.

The low fuel permeability of PPy does not exclude this material from further consideration as a catalyst support for FC electrodes. Nevertheless, it represents an important factor which has to be taken into the account. In order to design an efficient FC electrode PPy has to be used in the form of extremely thin layers modified by nanoparticles of catalyst deposited either on the mem-

brane surface or on the suitable gas diffusion layer. Such an arrangement assures sufficiently fast fuel transport to the catalyst surface and at the same time effective electron transport to the current collector.

6. Conclusions

The type of counter-ion influences the density and permeability of PPy films. The dense structure of PPy with small, divalent SO_4^{2-} results in low permeability. The incorporation of Nafion® with hydrophobic and hydrophilic domains into the structure of PPy significantly improves its permeability to hydrogen. This means that Nafion® is a promising counter-ion for PPy composites considered as a catalyst support for PEM FC. However, in general the relationship between the hydrophilicity/hydrophobicity and the size of the counter-ion and permeability is not yet completely clear and requires further investigation.

Acknowledgements

Financial support of this research by the Grant Agency of the Czech Republic under project number 104/02/0664 and by the European Union within the "Apollon" project, Project No. NNE5-2001-00187, is gratefully acknowledged.

References

1. T.R. Ralph and M.P. Hogarth, *Platinum metals Rev.* **46** (2002) 3.
2. Z. Qi, M.C. Lefebvre and P.G. Pickup, *J. Electroanal. Chem.* **459** (1998) 9.
3. X. Ren and P.G. Pickup, *J. Electroanal. Chem.* **396** (1995) 359.
4. C. Ehrenbeck and K. Jüttner, *Electrochimica Acta* **41** (1996) 1815.
5. D.A. Kaplin and S. Qutubuddin, *Polymer* **36** (1995) 1275.
6. H. Laborde, J.M. Léger and C. Lamy, *J. Appl. Electrochem.* **24** (1994) 219.
7. E.K.W. Lai, P.D. Beattie, F.P. Orfino, E. Simon and S. Holdcroft, *Electrochimica Acta* **44** (1999) 2559.
8. C. Coutanceau, M.J. Croissant, T. Napporn and C. Lamy, *Electrochimica Acta* **46** (2000) 579.
9. K. Bouzek, K.M. Mangold and K. Jüttner, *Electrochimica Acta* **46** (2000) 661.
10. K. Bouzek, K.M. Mangold and K. Jüttner, *J. Appl. Ectrochem.* **31** (2001) 501.
11. M.A. Del Valle, F.R. Díaz, M.E. Bodini, T. Pizarro, R. Córdova, H. Gómez and R. Schrebler, *J. Appl. Electrochem.* **28** (1998) 943.
12. M. Hepel, *J. Electrochem. Soc.* **145** (1998) 124.
13. P.J. Kulesza, M. Matczak, A. Wolkiewicz, B. Grzybowska, M. Galkowski, M.A. Malik and A. Wieckowski, *Electrochimica Acta* **44** (1999) 2131.
14. J. Shan and P.G. Pickup, *Electrochimica Acta* **46** (2000) 119.
15. M.J. Croissant, T. Napporn, J.M. Léger and C. Lamy, *Electrochimica Acta* **43** (1998) 2447.
16. A. Lima, C. Coutanceau, J.-M. Léger and C. Lamy, *J. Appl. Electrochem.* **31** (2001) 379.
17. H. Lee, J. Kim, J. Park, Y. Joe and T. Lee, *J. Power Sour.* **131** (2004) 188.
18. J. Park, J. Kim, H. Lee, T. Lee and Y. Joe, *Electrochimica Acta* **50** (2004) 769.
19. P. Chandrasekhar, *Conducting Polymers, Fundamentals and Applications* (Kluwer, Boston, 1999).
20. P. Burgmayer and J.V. Murray, *J. Phys. Chem.* **88** (1983) 2515.
21. G.S. Sauerbrey, *Z. Phys.* **155** (1959) 206.
22. G. Vatankhah, J. Lessard, G. Jerkiewicz, A. Zolfaghari and B.E. Conway, *Electrochimica Acta* **48** (2003) 1613.
23. K. Hyodo and M. Omae, *Electrochimica Acta* **35** (1990) 1245.
24. A. Michalska, U. Nadrzycka and K. Maksymiuk, *Fresenius*' J. Anal. Chem. **371** (2001) 35.
25. T.A. Skotheim, *Handbook of Conducting Polymers* 1 (Marcel Dekker, New York, 1986)pp. 91.
26. R.A. Bull, F.-R.F. Fan and A.J. Bard, *J. Electrochem. Soc.* **129** (1982) 1009.
27. J. Maruyama, M. Inaba, K. Katakura, Z. Ogumi and Z. Takehara, *J. Electroanal. Chem.* **447** (1998) 201.
28. K. Bouzek, P. Holzhauser, R. Kodym, S. Moravcova and M. Paidar, *J. Appl. Electrochem.* (2005) submitted.